A study on the function of the C-terminal half region of the Arf GTPase activating protein Gcs1p

A DISSERTATION

submitted to the Graduate School of Life Science,

Hokkaido University

in partial fulfillment of the requirements for the degree

DOCTOR OF LIFE SCIENCE

by

Zahra Zendehboodi

2013

CONTENTS

SUMMARY

ArfGAPs, GTPase-activating proteins for Arf small GTPases, are involved in multiple steps of vesicle formation of various transport pathways. Amphipathic Lipid Packing Sensor (ALPS) motif was first identified in the C-terminal regions of ArfGAP1 and its yeast homologue Gcs1p as a region that adsorbs preferentially onto highly curved membranes by folding into an amphipathic α-helix (AH). Previously it has been shown that Gcs1p functionally interacted with the phospholipid flippase Cdc50p-Drs2p in the early endosome-to-TGN retrieval pathway. In this study, I performed functional analyses of the C-terminal region of Gcs1p containing ALPS. Hydrophobic cluster analysis suggested that there is another potential AH-forming region downstream of ALPS in Gcs1p. Mutational analysis suggested that the ALPS motif is important for the Gcs1p function in the Golgi-to-ER retrograde pathway, whereas ALPS and the predicted AH region redundantly function in the post-Golgi pathways including the early endosome-to-TGN pathway. Liposome flotation assay indicated that this downstream region preferentially interacted with liposomes of smaller size. The region containing the ALPS motif was also required for the interaction with SNARE proteins including Snc1p and Tlg1p. These results suggest that ALPS and the predicted AH region are involved in the regulation and function of Gcs1p by interacting with membrane phospholipids and vesicle proteins.

ABBREVIATION

AH: amphipathic helix

ALPS: amphipathic lipid-packing sensor

Arf: ADP-ribosylation factor

COPI: coat protein I

CW: calcofluor white

DOPC: dioleoylphosphatidylcholine

DOPE: dioleoylphosphatidylethanolamine

DOPS: dioleoylphosphatidylserine

ER: endoplasmic reticulum

5-FOA: 5-fluoroorotic acid

GAP: GTPase-activating protein

GEF: guanine nucleotide exchange factor

GFP: green fluorescent protein

GST: glutathione *S*-transferase

HA: hemagglutinin

HCA: hydrophobic cluster analysis

IPTG: isopropyl-β-D-thio-galactoside

mutALPS: mutation of L246A, W250A, F253A

NBD-PE: 1-Palmitoyl-2-(6-NBD-aminocaproyl)-PE

PC: phosphatidylcholine

PE: phosphatidylethanolamine

PI: phosphatidylinositol

PS: phosphatidylserine

SD: synthetic medium

SDS-PAGE: sodium dodecyl sulfate polyacrylamide gel electrophoresis

SM: sphingomyelin

TGN: *trans*-Golgi network

t-SNARE: target membrane soluble *N*-ethylmaleimide-sensitive factor activating protein receptor

v-SNARE: vesicular soluble *N*-ethylmaleimide-sensitive factor activating protein receptor

INTRODUCTION

GTP-binding proteins of the ADP-ribosylation factor (ARF) family are important regulators of intracellular vesicle traffic. In the GTP-bound form, they associate with different sites of vesicle formation via insertion of their myristoylated N-terminal helix in the membranes to recruit coat proteins which promote sorting of cargo into vesicles. The function of this protein family is primarily controlled by guanine nucleotide exchange factors (GEFs), which catalyze GDP/GTP exchange and GTPase-activating proteins (GAPs), which induce GTP hydrolysis (1).

The yeast *S. cerevisiae* genome encodes four proteins with ArfGAP activity including Gcs1p, Glo3p, Age1p, and Age2p (2-5). Among them, Gcs1p which localizes to the endosomal/Golgi compartments, is the homologue of mammalian ArfGAP1 (12, 3, 6). ArfGAP1 has been shown to associate with curved membranes through two central ALPS (Amphipathic Lipid-Packing Sensor) motifs named ALPS1 and ALPS2 (7, 8) (Fig. 1). Gcs1p also contains a functional region homologous to ALPS1, but the existence of ALPS2 is unknown. The ALPS motif is supposed to be unstructured in solution, but forms an amphipathic helix upon contact with highly curved membranes. Because of enrichment of serine and threonine residues in the polar face of this motif, it cannot interact with polar region of the membranes using electrostatic effect, and therefore, adsorption of the ALPS motif depends exclusively on the insertion of its hydrophobic residues between lipids which is facilitated by defects in lipid packing upon introducing membrane curvature or conical lipids (7, 9).

Besides association with the membranes, Gcs1p induces conformational change on SNAREs, leading to recruitment of Arf1p and coatomer (10, 11). Like membrane curvature sensing by ALPS, Gcs1p interacted with SNAREs at its C-terminal region (12). However, exactly which

part of the C-terminal region is involved in the protein interaction has not been defined yet.

Previously, the functional relationship between Gcs1p and the Cdc50p-Drs2p in vesicle formation at the early endosomes has been reported (13). Cdc50p-Drs2p, in which Cdc50p and Drs2p are non-catalytic and catalytic subunits, respectively (14), is a member of the P4 subfamily of P-type ATPases (flippases), which is believed to mediate unidirectional transport of phospholipids including phosphatidylserine (PS) and phosphatidylethanolamine (PE) from the exoplasmic to cytoplasmic leaflet across the membrane lipid bilayers (15-18). In the plasma membrane of eukaryotic cells, PS and PE reside mainly in the cytoplasmic leaflet, while phosphatidylcholine (PC), sphingomyelin (SM), and glycosphingolipids are distributed on the opposite side. This lipid asymmetry has been supposed to be partly generated and maintained by flippases. In addition to the maintenance of lipid asymmetry, flippases are involved in vesicle formation possibly by generating membrane curvature through unidirectional transport of phospholipids to the cytosolic leaflet (19, 20). Cdc50p-Drs2p, which localizes mainly to the endosomal/TGN membranes, has been shown to have specific translocase activity toward PS, with a marginal effect on PE (21, 22). Accumulating evidence indicates that Cdc50p-Drs2p is involved in clathrin-coated vesicle-mediated protein transport in the TGN-early endosome bidirectional pathway (23). Consistently, in an earlier study, it has been found that the depletion of Cdc50p in *gcs1*Δ cells resulted in severe defects in the early endosome-to-TGN retrieval pathway (13). These findings suggest possible interplay between flippases and ArfGAPs harboring the ALPS motif in vesicle biogenesis.

Although the function of the GAP domain of Gcs1p has been well established, there is only limited knowledge of the potential roles of other portions in detail. In this study, I focus on the

role of the C-terminal half region of this protein as lipid- and protein-binding modules with an emphasis on the Cdc50p-Drs2p-mediated vesicle transport pathway. The ALPS motif was critical for the function redundant with the Glo3p GAP in the Golgi-to-ER retrograde pathway. In contrast, additional mutations or deletion in the potential amphipathic region downstream of the ALPS motif affected the function redundant with Cdc50p-Drs2p in the early endosome-to-TGN pathway. This region acts as a second lipid-packing sensor and along with the ALPS motif contributes to the membrane curvature sensitivity of Gcs1p. Also, I found that ALPS is involved in the interaction of Gcs1p with SNAREs Snc1p and Tlg1p. These results suggest that ALPS and the predicted AH region may contribute to the adaptation of the Gcs1p function for different transport pathways, possibly through their lipid- and protein-binding dual-specificity.

MATERIALS AND METHODS

Media and genetic methods-Strains were grown in YPDA rich medium (1% Bacto-yeast extract [Difco, Detroit, MI], 2% Bacto-peptone [Difco], 2% glucose, and 0.01% adenine). Strains carrying plasmids were selected in synthetic medium (SD) containing the required nutritional supplements (24). When appropriate, 0.5% casamino acids (Difco) were added to SD medium without uracil or tryptophan (SDA-Ura or SDA-Trp). For induction of the *GAL1* promoter, 3% galactose and 0.2% sucrose were used as carbon sources instead of glucose (YPGA). Calcofluor white (CW) sensitivity was tested on a YPDA plate containing 100 μg/ml CW (Sigma-Aldrich, St Louis, MO, USA). SD plates containing 0.1% 5-fluoroorotic acid (5-FOA; Wako Pure Chemicals, Osaka, Japan) were used to counterselect the presence of *URA3*-containing plasmids. Standard genetic manipulations of yeast were performed as described previously (25). Yeast transformations were performed using the lithium acetate method (26, 27).

Strains and plasmids-Yeast strains used in this study are listed in Table I. *GAL1* promoter-inducible *GLO3* and *AGE2* were constructed by polymerase chain reaction (PCR)-based procedures as described previously (28). The constructs were verified by colony-PCR amplification to confirm that the integrations had occurred at the expected loci. The *chs6*Δ strains harboring *gcs1*Δ, *glo3*Δ, or *age2*Δ were constructed by a cross of YKT1656 (*chs6*Δ*::KanMX4)* with YKT1631 (*gcs1*Δ*::HphMX4*), YKT1763 (*glo3*Δ*::HphMX4*), or YKT1764 (*age2*Δ*::HphMX4*) respectively, followed by tetrad dissection.

Plasmids used in this study are listed in Table II. *Escherichia coli* strains XL1-Blue and DH5α were used for the construction and amplification of plasmids and the expression and

purification of GST-fused proteins, respectively. *GCS1* alleles containing point mutations were created using a QuikChange site-directed mutagenesis kit (Stratagene, La Jolla, CA) and verified by sequencing. Schemes detailing the construction of plasmids and DNA sequences of nucleotide primers are available on request.

Microscopic observations-Cells were observed using a Nikon ECRIPSE E800 microscope (Nikon Instec, Tokyo, Japan) equipped with an HB-10103AF super high-pressure mercury lamp and a 1.4 numerical aperture 100x Plan Apo oil immersion objective with the appropriate fluorescence filter sets and differential interference contrast (DIC) optics. Images were acquired with a digital cooled charge-couple device camera (C4742–95-12NR; Hamamatsu Photonics, Hamamatsu, Japan) by using AQUACOSMOS software (Hamamatsu Photonics). Observations are compiled from the examination of at least 100 cells.

To visualize GFP-Snc1p in living cells, cells were grown at 14ºC for more than 18 h, harvested, and resuspended in SD medium. Cells were mounted on the microslide glass and observed immediately using a GFP (green) bandpass filter set. To examine the localization of GFP-Snc1p in fixed cells (Fig. 4), cells were grown at 30°C to early-mid logarithmic phase, followed by incubation in synthetic medium containing glucose. After repression of the *GAL1* promotor for 7 h, cells were fixed by addition of a commercial 37% formaldehyde stock (Wako Pure Chemicals) into the medium to a final concentration of 1%, followed by a 10 min incubation at 30°C, and then, washed twice with phosphate-buffered saline and observed. Ultrastructural observation of cells by conventional electron microscopy was performed using

the glutaraldehyde-osmium fixation technique according to procedures described previously (13).

Lipid preparation-Dioleoylphosphatidylcholine (DOPC), dioleoylphosphatidylethanolamine (DOPE), dioleoylphosphatidylserine (DOPS), liver phosphatidylinositol (PI), cholesterol, and 1-Palmitoyl-2-(6-NBD-aminocaproyl)-PE (NBD-PE) were obtained from Avanti Polar Lipids (Alabaster, AL). The (C18:1-C18:1) Golgi-mix liposomes were prepared as described previously (7). Briefly, the indicated lipids were mixed in chloroform at the composition of (mol %) DOPC (50), DOPE (19), DOPS (5), PI (10), cholesterol (16), and NBD-PE (0.2). Chloroform was removed by evaporation followed by vacuum desiccation. The resulting dried film was resuspended in HKM buffer (50 mM HEPES·KOH, pH 7.2, 120 mM potassium acetate, 1 mM $MgCl_2$) to a final concentration of 2 mM lipids, followed by five steps of thawing and freezing in liquid nitrogen. To produce defined size vesicles, the liposome suspension was passed sequentially through a LiposoFast-Basic stabilizer (Avestin, Ottawa, Canada), equipped with polycarbonate filters with pore sizes of 1.0, 0.8, 0.4, 0.1, 0.05, and 0.03 μm. The mean liposome radius was estimated by dynamic light scattering using Fiver-Optical Light-Scattering Spectrophotometer (FDLS-3000; Otsuka Electronics, Osaka, Japan)

Protein expression and purification-All GST-fused constructs were expressed under the control of the *tac* promoter. The *E. coli* cells were grown at 37°C to a cell density of ~0.8 OD_{600}/ml, shifted to 20°C, and cultured for about 12 h in the presence of 100 μM IPTG. After protein production, bacteria were washed with phosphate-buffered saline, and then lysed in H

buffer (50 mM HEPES·KOH, pH 8.0 at 4°C, 1 mM EDTA, 1 mM EGTA, and 10% sucrose) supplemented with protease inhibitors (2 μg/ml aprotinin, 2 μg/ml leupeptin, and 1 mM phenylmethylsulfonyl fluoride). The supernatant was loaded onto 0.5 ml bed volume of glutathione Sepharose 4B column (GE Healthcare, Uppsala, Sweden). The column was washed twice with five bed volumes of HKM buffer, pH 8.0 at 4°C, and eluted with the same buffer supplemented with 10 mM reduced glutathione (Wako Pure Chemicals). A portion of each eluted protein was subjected to SDS-PAGE, followed by staining with SYPRO red (Lonza, Basel, Switzerland) and the concentration of recovered GST-fused proteins was estimated by densitometry with a FUJI FLA-3000 fluorescent image analyzer (Fuji Photo Film, Tokyo, Japan), using bovine serum albumin as a reference protein.

Liposome flotation experiments-Proteins (1.5 μM) were mixed with liposomes (1 mM) of defined radii in HKM buffer at pH 7.2 in a total volume of 150 μl, followed by incubation at room temperature for 5 min. To prepare sucrose layers, 100 μl of a 75% (w/v) sucrose solution in HKM buffer was added to the protein-liposome mixture to obtain a 30% (w/v) sucrose suspension. The resulting high-sucrose suspension was overlaid with two cushions of lower density, 250 μl of HKM containing 25% (w/v) sucrose and 50 μl of HKM containing no sucrose. As a control, a similar experiment was performed without liposome. The samples were centrifuged at 55,000 rpm (240,000 × g) for 1 h using a TLS55 swing rotor (Beckman, Brea, CA). After centrifugation, the bottom (250 μl), middle (150 μl) and top (150 μl) fractions were separated and then subjected to SDS–PAGE followed by SYPRO red staining. The protein content of each band was quantified by the FLA-3000 fluorescence imaging system using a

GST-Gcs1p(mutALPS/F292A/F296A) protein as a standard. The recovery of the liposomes during centrifugation and after fraction collection was confirmed by following NBD-PE fluorescence.

Antibodies-The mouse anti-HA (16B12) and -myc (9E10) monoclonal antibodies were purchased from COVANCE (Princeton, NJ). The horseradish peroxidase (HRP)-conjugated secondary antibodies (sheep anti-mouse IgG and donkey anti-rabbit IgG) used for immunoblotting were purchased from GE Healthcare. Polyclonal anti-GST antibodies were affinity-purified by passing anti-serum against GST-Cdc50p (29) over a column of GST coupled to CNBr-activated Sepharose 4B.

*Snc1p/Tlg1p-Gcs1p binding assay-gcs1*Δ cells (YKT1768) harboring pRS416-3HA-SNC1 (pKT1564) or pRS416-2HA-TLG1 (pKT2052) were grown at 30°C to a cell density of ~1.2 OD_{600}/ml in SDA-Ura medium. Cells collected from 600 ml of the cultures were washed once with ice-cold water and resuspended at 200 OD_{600}/ml in lysis buffer (50 mM HEPES·KOH, pH 7.5 at 4°C, 0.3 M sorbitol, 150 mM NaCl, and 5 mM EDTA) containing protease inhibitors (2 μg/ml leupeptin and 1 mM phenylmethylsulfonyl fluoride). The cells were lysed by Multi-beads shocker (Yasui Kikai, Osaka, Japan). Cell lysates were centrifuged at 400 × *g* for 5 min, and the resulting supernatant was centrifuged at 100,000 × *g* for 1 h at 4°C (TLA120.2 rotor; Beckman). The supernatant was removed to obtain a pellet of total membranes. For immunoprecipitation of 3HA-Snc1p or 2HA-Tlg1p, membrane pellets were solubilized in 0.65 ml of immunoprecipitation buffer (50 mM HEPES·KOH, pH 7.5 at 4°C, 150 mM NaCl, 5 mM EDTA,

and 1% 3-[(3-cholamidopropyl) dimethylammonio]propanesulfonate (CHAPS)) containing the above-mentioned protease inhibitors. After rotating at 4°C for 30 min, the suspension was centrifuged at 12,000 rpm for 10 min and the supernatant was separated from insoluble materials. The supernatant was incubated with 30 μg of anti-HA antibody for 2 h at 4°C with rotating. As a control, the same experiment was performed using a lysate containing GFP-Snc1p or GFP-Tlg1p. These samples were then rotated with 60 μl of protein G-Sepharose 4 Fast Flow (GE Healthcare) for 2 h at 4°C. The protein G-Sepharose beads were then pelleted, and washed three times with binding buffer (50 mM HEPES·KOH, pH 7.5 at 4°C, 150 mM NaCl, 5 mM EDTA, and 0.5% CHAPS) containing the above-mentioned protease inhibitors. Then 10 μl of beads was mixed with 100 μl of 0.75 μM of GST-fused Gcs1p(221-352aa) versions in the binding buffer, and the resulting mixture was incubated at 4°C for 1 h. After pelleting and washing the beads, the immunoprecipitates were separated by SDS-PAGE and transferred to polyvinylidene difluoride membrane. Membranes were blocked in 5% skim milk in 50 mM Tris-HCl, pH 7.5, 200 mM NaCl with 0.05% Tween 20 (TBST) for 1 h at room temperature. Membranes were then incubated with primary antibody (anti-HA antibody diluted 1:1000 or anti-GST antibody diluted 1:1000 in 5% skim milk in TBST) for 2 h at room temperature. After washing and blocking in 5% skim milk in TBST, the membrane was incubated with secondary antibody (anti-mouse IgG-HRP or anti-rabbit IgG-HRP diluted 1:1000 in TBST) for 2 h at room temperature. After three washes in TBST, protein bands were detected by chemiluminescence (ECL, GE Healthcare) using LAS1000plus (Fuji Photo Film).

RESULTS

The ALPS motif is essential for the Gcs1p function in the Golgi-ER retrograde transport pathway-Although the existence of a region homologous to ALPS1 of ArfGAP1 has been reported in Gcs1p, sequence alignment of Gcs1p and ArfGAP1 showed that there is no any region homologous to ALPS2 in this protein (8). However, the HCA (Hydrophobic Cluster Analysis) plot and helical wheel projections revealed that the downstream region of the ALPS motif also has a suggestive feature of amphipathic helix (AH) structure (Fig. 1). In this regard, in addition to investigating the importance of the ALPS motif, I was interested to know if, like ArfGAP1, the predicted AH region downstream of ALPS has a potential function. Gcs1p functions redundantly with two other ArfGAPs, Glo3p and Age2p in the Golgi-to-ER retrograde transport pathway and in transport from the TGN, respectively (4, 5). Therefore, as a first approach, I genetically determined the importance of ALPS and the predicted AH region in these pathways. To this end, I constructed various deletion derivatives of Myc-tagged Gcs1p, which were lacking the ALPS motif (228-279 a.a.), the predicted AH region (281-311 a.a.), or both (Fig. 2A). I also mutated three conserved hydrophobic residues of ALPS (L246, W250, F253) simultaneously to alanine (mutALPS). These residues of ArfGAP1 make an essential contribution of ArfGAP1 to the recognition of curved membrane (7). To examine the possible forming of AH, as a first proposed function for the predicted AH region, some hydrophobic residues in this region (L281, F292, F296) were also replaced individually (L281A) or in combination (F292A/F296A) by alanine. Double mutations of ALPS and the predicted AH region were created too. The constructed Gcs1p versions were expressed at a level comparable to that of wild type under the control of the native promoter from a low copy plasmid (Fig. 2B).

The Gcs1p mutant derivatives were introduced into P_{GAL1}-*GLO3 gcs1*Δ and P_{GAL1}-*AGE2 gcs1*Δ mutant strains and the growth property was examined using repressing (glucose) and inducing (galactose) conditions of *GAL1*-promotor. As shown in Fig. 3A, deletion or point mutation of the ALPS motif alone, but not the predicted AH region, failed to support the growth of Glo3p-depleted *gcs1*Δ cells. This result reveals that ALPS is specifically critical for the Gcs1p function redundant with Glo3p in the Golgi-ER retrograde transport pathway. In contrast, Age2p-depleted *gcs1*Δ cells showed genetic interaction only with double mutant of Gcs1p, which contain mutations in both ALPS and the predicted AH region, although the growth defect was weak (Fig. 3B). It has been reported that the lethality of *gcs1*Δ *age2*Δ double-mutant cells can be circumvented by increased abundance of the Age1p ArfGAP (30). In that regard, in the post-Golgi transport pathway, physiological dosage of Age1p may be enough to overcome the functional defects of the Gcs1p versions, which were not mutated severely. Nonetheless, these data indicate the redundancy of ALPS and the predicted AH region for Gcs1p function in the post-Golgi transport pathway.

The ALPS motif and the predicted AH region of Gcs1p have the redundant function in the early endosome-to-TGN transport pathway-I next determined the importance of ALPS and the predicted AH region for the functional relationship of Gcs1p with Cdc50p in the retrieval pathway from the early endosome to the TGN. For this, the P_{GAL1}-*CDC50 gcs1*Δ mutant strain was transformed with Gcs1p derivatives and examined as in Fig. 3. Deletion of either the ALPS motif (Δ228-279) or the predicted AH region (Δ281-311) did not cause any growth defect of the Cdc50p-depleted cells, whereas deletion of both of them (Δ228-315) exhibited the severe defect

similar to the null mutation (Fig. 4A). These data suggest that ALPS and the predicted AH region are functionally redundant for the growth in the Cdc50p-depleted condition. These results were reproduced with point mutations: only the combination of mutALPS and F292A/F296A mutations caused the severe growth defect of Cdc50p-depleted cells. However, mutALPS did not exhibit the synthetic defect with the L281A mutation.

I also investigated the effect of *GCS1* mutations on the endocytic recycling pathway that is the early endosome-to-TGN pathway using GFP-Snc1p as a marker protein. Snc1p, an exocytic v-SNARE, is mainly localized to actively growing sites such as the bud plasma membrane. After fusion of vesicles with the plasma membrane, Snc1p is endocytosed and recovered through the endocytic recycling pathway (31). Thus, in mutants in this pathway, GFP-Snc1p is intracellularly accumulated. When Cdc50p was partially depleted for 7 h, GFP-Snc1p was normally localized to the plasma membrane in 89% of the cells (WT, n=130), whereas in the Ccd50p-depleted *gcs1*Δ mutant cells, it did so only in 1.7% of the cells (Vector, n=116) (Fig. 4B). Expression of mutALPS, F292A/F296A and L281A in this Ccd50p-depleted *gcs1*Δ mutant restored normal localization of GFP-Snc1p in 60% (n=136), 39% (n=121), and 40% (n=146) of the cells, respectively. In contrast, mutALPS/F292A/F296A did not restore GFP-Snc1p localization (4%, n=117). The versions of Gcs1p harboring deletion of ALPS motif or/and the predicted AH region also represented the similar phenotypes.

Previously it has been shown that the Cdc50p-depleted *gcs1*Δ cells accumulated many of large abnormal double membrane structures with crescent- or ring-shaped morphologies similar to what were observed in *cdc50*Δ and *drs2*Δ mutants grown at a low temperature by electron microscopy (13). These structures are supposed to be excessive early endosomal membranes,

which may have been arisen due to defective formation of vesicles from early endosomes. When Cdc50p was partially depleted for 7 h, the F292A/F296A and mutALPS/F292A/F296A mutations caused accumulation of these structures in 10-20% and 80-90% of the sections, respectively (Fig. 4C). The mutALPS single mutation did not cause major defects in Cdc50p-depleted *gcs1*Δ cells. The severer phenotypes with the F292A/F296A mutation compared to the mutALPS mutation were also observed in the cell growth and recycling of GFP-Snc1p (Fig. 4A and B). Taken together, these results reflect the importance of both ALPS and the predicted AH region, likely in aspect of their membrane binding abilities through hydrophobic residues, for the correct functional relationship of Gcs1p with Cdc50p *in vivo*.

The functional importance of the ALPS motif and predicted AH region in the early endosome-to-TGN pathway was further confirmed by two different experiments as follows. Tlg2p is a t-SNARE, which is involved in recycling of proteins from the early endosome to the TGN (31). The *tlg2*Δ mutation exhibited synthetic lethality with *cdc50*Δ (32) and *gcs1*Δ (12). *GCS1* mutant derivatives were examined for suppression of the lethality of the *tlg2*Δ *gcs1*Δ mutant. I found almost the same pattern of genetic interaction in these experiments with that of Cdc50p-depleted condition (Fig. 5).

At lower temperatures such as 15ºC, the *gcs1*Δ mutant exhibits growth defects (12, 33) and intracellularly accumulates GFP-Snc1p (13). The C-terminal truncated mutant of Gcs1p exhibited a substantial growth defect, whereas a little growth defect was observed with Δ228-315 and mutALPS/F292A/F296A mutations at 14ºC (data not shown). Consistently, the *gcs1* Δ*228-315* and *mutALPS/F292A/F296A* mutants totally or partially accumulated GFP-Snc1p in 54% (n=114) and 76% (n=114) of the cells, respectively at 14°C (Fig. 6).

Mutations in the ALPS motif and the predicted AH region of Gcs1p affect the intracellular retention of Chs3p-Chitin synthase III (Chs3p), an enzyme involved in the assembly of the cell wall chitin at the mother-bud junction, cycles from the plasma membrane through the early endosome/TGN to the cell surface. The Chs5p and Chs6p coat complex is essential for the transport of Chs3p from the TGN to the plasma membrane (34, 35). Since chitin renders cells sensitive to the chitin binding dye calcofluor, the cells lacking *CHS5* or *CHS6* are resistant to calcofluor. It was shown that disruption of the clathrin adaptor protein complex 1 (AP-1), *CHC1* (clathrin heavy chain), and *ARF1* bypass the *chs6*Δ defect and restored calcofluor sensitivity, suggesting that in the absence of these genes, Chs3p is rerouted to the plasma membrane possibly from early endosomes due to the blockade in the early endosome-to-TGN pathway (36). This suppression was also observed with the *drs2*Δ mutation, suggesting that AP-1 and Cdc50p-Drs2p function in a common pathway (37).

To investigate the role of ArfGAPs in this pathway, I first assessed the ability of *gcs1*Δ, *glo3*Δ and *age2*Δ to bypass the *chs6*Δ defect. The *gcs1*Δ mutation restored calcofluor sensitivity of *chs6*Δ cells (Fig. 7A). This observation is in agreement with the role of Gcs1p in the early endosome-to-TGN pathway. Interestingly, deletion of *AGE2* and *GLO3* also restored calcofluor sensitivity, although the effect of *glo3*Δ was not as strong as the other two GAPs. These results suggest that Age2p and Glo3p are also involved in trafficking of Chs3p directly or indirectly. Next, to examine the specific role of ALPS and the predicted AH region in the transport of Chs3p, I explored the effect of Gcs1p versions on the calcofluor sensitivity of the cells with the *chs6*Δ *gcs1*Δ background. The results were almost the same with those of the Cdc50p-depleted

condition (Fig. 7B). These results are most consistent with the idea that the predicted AH region downstream of the ALPS motif is important together with the ALPS motif in the early endosome-to-TGN pathway.

The predicted AH region downstream of ALPS can recognize membrane curvature-The ALPS motif of Gcs1p, like that of ArfGAP1, has been reported to respond to membrane curvature (7). However, more details of the lipid binding property of this region, and also the possible same function carried by the predicted AH region, as our *in vivo* observations suggest, have still remained to be clarified. To address this, I first assessed the lipid-interacting property of the ALPS motif in combination with the predicted AH region. For this, the *E.coli* plasmid expressing a truncated form of Gcs1p, Gcs1p(221-352), in a fusion with GST was constructed. The mutant versions of this construct harboring mutALPS, F292A/F296A, or their combination were also created. Then ability of the purified proteins to bind to Golgi-mix liposomes of a defined size was assessed by liposome flotation assay as described in Materials and Methods. The (C18:1-C18:1) Golgi-mix liposomes contained DOPC (50), DOPE (19), DOPS (5), PI (10), and cholesterol (16) (mol %) (7). In these experiments, liposomes and their bound proteins move to the top (T) fraction from the bottom (B) fraction after centrifugation, whereas unbound proteins are left in the bottom fraction. As shown in Fig. 8A, a significant amount (73%) of the wild type form was recovered by 46 nm liposomes, while the amounts recovered by the liposomes of larger size were also noticeable (58% for 70 nm and 49% for 137 nm). A previous study showed that Gcs1p bound to small size liposomes with clearer specificity (7). This discrepancy might be due to the difference of the Gcs1p fragment used: the previous study used

the full-length Gcs1p, whereas I used GST-fused ALPS and the predicted AH region.

The mutALPS mutation sharply weakened the affinity of membrane binding with large size liposomes (15% for 70 nm and 10% for 137 nm), suggesting that this binding is dependent on the ALPS motif. In contrast, there was still substantial binding to the 46 nm liposomes with mutALPS (60%). Although I did not examine the liposome binding property of the isolated ALPS, a previous observation for ArfGAP1 showed that the mutALPS mutation in the same residues drastically decreased the membrane curvature sensitivity of ALPS1 regardless of liposome size (7). Given this, my data might point to the compensatory effect of the predicted AH region in the recognition of small size liposomes. In fact, adding the F292A/F296A mutation decreased the binding to small size liposomes to 21%. The F292A/F296A mutation alone did not alter the adsorption property, suggesting that the ALPS motif is the major determinant of the association of Gcs1p with curved membranes.

I next examined the dose-dependent binding of above derivatives to the 37 nm liposomes (Fig. 8B). Similar to the wild type, the F292A/F296A mutant exhibited dose-dependent binding, suggesting that ALPS is enough for this binding. The ALPS mutated version also bound in a dose-dependent manner, albeit less efficiently. However, the binding of mutALPS/F292A/F296A was dose-independent, suggesting that its weak binding to small liposomes was non-specific. These results suggest that the predicted AH region also binds to small liposomes in a specific manner. Thus, I wished to further determine the lipid binding capability of the predicted AH region individually. To this end, the GST-fused Gcs1p(280-352) and its mutated version for F292A/F296A were constructed and examined as described in Fig. 8A using liposomes of 41 and 145 nm. For comparison, Gcs1p(221-352) and its F292A/F296A mutated form used in Fig. 8A

were also included. As shown in Fig. 8C, Gcs1p(280-352) weakly but specifically bound to small liposomes (38%), and the F292A/F296A mutation completely abrogated the adsorption, suggesting the importance of hydrophobic residues of this domain in the sensing of curved membranes, as what were observed for the ALPS of Gcs1p and also the ALPS motifs of other proteins (7, 8, 38). Together, these results support the conclusion that like ArfGAP1, there is a second ALPS-like domain, which contributes together with the ALPS to the adsorption of Gcs1p by lipid membranes.

Previous works on the proteins with different types of AHs have shown that, unlike the proteins containing ALPS motif which is adapted to curved membranes with low amounts of anionic lipids, α-synuclein, a protein involved in neurodegenerative diseases, contains an AH which uses both membrane curvature and anionic lipids to associate with the membranes (39). Because Drs2p was shown to preferentially transport a fluorescence-labeled PS (21, 40), the genetic interaction between *GCS1* and *CDC50* might suggest that the ALPS motif of Gcs1p requires anionic phospholipids for interaction with liposomes. Given this, I examined the effect of PS depletion on the lipid sensitivity of Gcs1p(221-352). I carried out flotation assay using Golgi-mix liposomes of defined size, in which DOPS was removed at the expense of DOPC. However, in agreement with previous observations for other ALPS motifs (7, 38, 39), I did not find a significant change in the ability of Gcs1p constructs to the PS-lacking liposomes of any size (Fig. 9).

The ALPS motif also contributes to the interaction of Gcs1p with Snc1p and Tlg1p-It was previously reported that Snc1p and its homolog Snc2p physically interacted with the C-terminal

region of Gcs1p including the ALPS motif and the predicted AH region (12). Since Gcs1p induced a conformational change on both v- and t-SNAREs to promote v-t-SNARE complex formation of ER-Golgi SNAREs *in vitro* (11), there would be a possibility that Gcs1p interaction is not confined to v-SNAREs, but also it could be extended to t-SNAREs as well. To address this possibility, I investigated the physical interaction of Tlg1p and the C-terminal half region of Gcs1p *in vitro*. Tlg1p is a t-SNARE, which together with Tlg2p is involved in the recycling of TGN proteins from early endosomes (31). The membrane protein extracts prepared from the cells expressing 3HA-Snc1p or 2HA-Tlg1p were subjected to immunoprecipitation with an anti-HA antibody and then the immunoprecipitates were incubated with purified GST-fused Gcs1p(221-352). The protein complexes were then immunoblotted with anti-HA and -GST antibodies. I found that GST-fused Gcs1p(221-352) coprecipitated with 2HA-Tlg1p as well as 3HA-Snc1p (Fig. 10). Next, to elucidate if the ALPS motif and the predicted AH region are important for interaction with 3HA-Snc1p or 2HA-Tlg1p, the same experiment as described above was performed with purified GST-fused Gcs1p(221-352) mutant derivatives. As shown in Fig. 10, the mutALPS mutation inhibited the interaction with 3HA-Snc1p and 2HA-Tlg1p. The F292A/F296A mutations also caused a little reduction in the interaction. I also obtained essentially the same results for interaction with Snc1p using two-hybrid assay (data not shown). These observations, in conjunction with the above-described results of the flotation assay, suggest that the lipid-binding domain of Gcs1p overlaps with its protein-binding domain, and that both interactions are mediated mainly through hydrophobic effects.

DISCUSSION

The function of the ALPS motif and the predicted AH region in the pre- and post-Golgi transport pathways-In the present study, I demonstrate that the ALPS motif and the predicted AH region are essentially important for the Gcs1p function. As the summary of genetic interaction showed (Table III), the existence of ALPS, but not the predicted AH region, is inevitable for the Gcs1p function redundant with Glo3p. In contrast, either the ALPS motif or the predicted AH region is sufficient for the Gcs1p function redundant with Cdc50p-Drs2p or Age2p. The different behavior of Gcs1p in the pre and post-Golgi pathways might be explained by a different lipid environment of these pathways. As it has been reported, membranes in the post-Golgi secretory pathways contain high surface charge and tight lipid packing, whereas those in the early secretory pathways contain low surface charge and loose lipid packing (41). My data of liposome-binding assay revealed that the ALPS motif and the predicted AH region exhibit different property of membrane recognition. That is, the ALPS motif was the primary determinant in the recognition of membranes and can associate with less curved membranes at least in my experimental conditions, while the predicted AH region was less important but had a compensatory activity to sense the small size liposomes. Supposedly, the ALPS motif may take advantage of loose lipid packing of the pre-Golgi membranes regardless of the degree of curvature, while the predicted AH region might not be satisfied with the space level of these surfaces. Further studies are required to clarify the behavior of Gcs1p to different lipid environments in more detail.

Although the post-Golgi lipid environments seem to be tight, the flippases present at these membranes may modulate the lipid packing by expanding the cytoplasmic leaflet, in expense of

decreasing the number of phospholipids in the luminal leaflet, and therefore, they may produce a local membrane bending with enough space at the site of vesicle formation which could allow the predicted AH region to be absorbed. Interestingly, the predicted AH region was more important than the ALPS motif in the early endosome-to-TGN pathway (Fig. 4, 5, and 7). This region might be more adapted to the recognition of membrane curvature created by the action of flippases. The functional relationship of Cdc50p-Drs2p with Gcs1p, but not with Age2p, may further support this idea (13). Age2p, which could not compensate for Gcs1p in the absence of Cdc50p-Drs2p, has not been reported to have a domain like the ALPS motif. These findings may point to the cooperation of flippases, in regard of creating the membrane curvature, and the proteins with curvature sensing ability in the flippase-dependent trafficking pathway. Drs2p was shown to preferentially transport a fluorescence-labeled PS (21, 40). However, PS depletion did not affect the binding of the ALPS motif and predicted AH region to liposomes (Fig. 9). Drs2p is required for cell growth in the *cho1* mutant, which completely lacks PS, suggesting that Drs2p transports another phospholipid in addition to PS (21). Thus, the ALPS motif and predicted AH region may also recognize PE or PC in the absence of PS or they can interact with membranes in a head group-independent manner.

Involvement of ArfGAPs in the traffic of Chs3p-Previously, it has been shown that Cdc50p-depleted *gcs1*Δ mutant cells accumulated Chs3p in aberrant membrane structures, which were colocalized with Snc1p (13). The present study confirms this observation as *gcs1*Δ bypassed the *chs6*Δ defect possibly through the blocking of Chs3p retrieval from the early endosome to the TGN, which results in transport of Chs3p to the plasma membrane via an

unknown route (36). Contrary to the idea of the redundant function of Age2p and Gcs1p in the early endosome-to-TGN retrieval pathway (30), my results revealed that these two GAPs could not compensate for each other in the retrograde transport of Chs3p. These findings may reflect the necessity of each GAP individually or defined dosage of ArfGAPs in general for transport of Chs3p.

As to the weak suppression by *glo3*Δ, one possibility is that in the absence of Glo3p, the concentration of Gcs1p at the early endosome may decrease due to compensation for Glo3p at the early Golgi. An alternative possibility, as proposed by Graham's group for the suppression by AP-1 mutation, is that the suppression by *glo3*Δ could occur at the TGN level (37). Glo3p has been shown to be a component of COPI-coated vesicles and it interacted genetically and physically with the coatomer protein Sec21p. *glo3*Δ cells are impaired for vesicular transport not only in the Golgi-to-ER retrograde pathway, but also in the ER-to-Golgi anterograde pathway: defective retrieval of components necessary for anterograde transport causes the indirect effect of *glo3*Δ on this pathway (4, 42). Therefore, suppression by *glo3*Δ may happen at the TGN, perhaps due to defective transport of the components, which are required for the early endosome-to-TGN transport of Chs3p, from the TGN to the early endosome, resulting in rerouting of Chs3p to the plasma membrane.

ALPS and the predicted AH region function as lipid and protein interaction modules-The function of ArfGAPs is not limited to terminators of Arf1p. Otherwise, recent studies have revealed that they perform multiple actions in the membrane traffic; they function as the Arf effectors and coat components, and are possibly involved in vesicle fission and vesicle uncoating

(43). My data revealed that the ALPS motif contributed to both lipid and protein interaction, suggesting that the two binding sites overlap significantly. This overlap is possibly to have a functional importance. Lipid- and protein-binding dual-specificity modules have been reported for some protein with PDZ (a small modular protein-interaction domain) or PTB (phosphotyrosine binding) domains. In some of these domains, protein and lipid interaction sites are overlapped, and in some of PDZ domains, protein interaction is regulated by lipid binding (44, 45).

The dual specificity property of ALPS may be beneficial for Gcs1p function. For instance, in the beginning of vesicle formation, Gcs1p may associate with transmembrane proteins such as SNAREs via the ALPS motif. This interaction makes SNAREs to undergo a conformational change, and subsequently, Arf1p is recruited to the site of vesicle formation (10, 12). During vesicle formation, when the membrane is converted to the curved shape with the aid of a flippase, the ALPS motif may preferentially shift Gcs1p from the SNAREs to the curved membrane, which therefore enables Gcs1p to promote GTP hydrolysis by Arf1p (Fig. 11). Taken together, my study revealed that, like ArfGAP1, Gcs1p is a multifunctional protein, which in addition to the GAP-dependent activity, facilitates the membrane trafficking in different pathways through its non-GAP domains possibly specialized for distinct functions.

REFERENCES

1. Donaldson, J. G., and Jackson, C. L. (2011) ARF family G proteins and their regulators: roles in membrane transport, development and disease. *Nat. Rev. Mol. Cell Biol.* **12**, 362-375

2. Zhang, C. J., Bowzard, J. B., Anido, A., and Kahn, R. A. (2003) Four ARF GAPs in *Saccharomyces cerevisiae* have both overlapping and distinct functions. *Yeast* **20**, 315-330

3. Poon, P. P., Wang, X., Rotman, M., Huber, I., Cukierman, E., Cassel, D., Singer, R. A., and Johnston, G. C. (1996) *Saccharomyces cerevisiae* Gcs1 is an ADP-ribosylation factor GTPase-activating protein. *Proc. Natl. Acad. Sci. USA* **93**, 10074-10077

4. Poon, P. P., Cassel, D., Spang, A., Rotman, M., Pick, E., Singer, R. A., and Johnston, G. C. (1999) Retrograde transport from the yeast Golgi is mediated by two ARF GAP proteins with overlapping function. *EMBO J.* **18**, 555-564

5. Poon, P. P., Nothwehr, S. F., Singer, R. A., and Johnston, G. C. (2001) The Gcs1 and Age2 ArfGAP proteins provide overlapping essential function for transport from the yeast trans-Golgi network. *J. Cell Biol.* **155**, 1239-1250

6. Cukierman, E., Huber, I., Rotman, M., and Cassel, D. (1995) The ARF1 GTPase-activating protein: zinc finger motif and Golgi complex localization. *Science* **270**, 1999-2002

7. Bigay, J., Casella, J. F., Drin, G., Mesmin, B., and Antonny, B. (2005) ArfGAP1 responds to membrane curvature through the folding of a lipid packing sensor motif. *EMBO J.* **24**, 2244-2253

8. Mesmin, B., Drin, G., Levi, S., Rawet, M., Cassel, D., Bigay, J., and Antonny, B. (2007) Two lipid-packing sensor motifs contribute to the sensitivity of ArfGAP1 to membrane curvature. *Biochemistry* **46**, 1779-1790

9. Antonny, B., Huber, I., Paris, S., Chabre, M., and Cassel, D. (1997) Activation of ADP-ribosylation factor 1 GTPase-activating protein by phosphatidylcholine-derived diacylglycerols. *J. Biol. Chem.* **272**, 30848-30851

10. Rein, U., Andag, U., Duden, R., Schmitt, H. D., and Spang, A. (2002) ARF-GAP-mediated interaction between the ER-Golgi v-SNAREs and the COPI coat. *J. Cell Biol.* **157**, 395-404

11. Schindler, C. and Spang, A. (2007) Interaction of SNAREs with ArfGAPs precedes recruitment of Sec18p/NSF. *Mol. Biol. Cell* **18**, 2852-2863

12. Robinson, M., Poon, P. P., Schindler, C., Murray, L. E., Kama, R., Gabriely, G., Singer, R. A., Spang, A., Johnston, G. C., and Gerst, J. E. (2006) The Gcs1 Arf-GAP mediates Snc1,2 v-SNARE retrieval to the Golgi in yeast. *Mol. Biol. Cell* **17**, 1845-1858

13. Sakane, H., Yamamoto, T., and Tanaka, K. (2006) The functional relationship between the Cdc50p-Drs2p putative aminophospholipid translocase and the Arf GAP Gcs1p in vesicle formation in the retrieval pathway from yeast early endosomes to the TGN. *Cell Struct. Funct.* **31**, 87-108

14. Saito, K., Fujimura-Kamada, K., Furuta, N., Kato, U., Umeda, M., and Tanaka, K. (2004) Cdc50p, a protein required for polarized growth, associates with the Drs2p P-Type ATPase implicated in phospholipid translocation in *Saccharomyces cerevisiae*. *Mol. Biol. Cell* **15**, 3418-3432

15. Daleke, D. L. (2007) Phospholipid flippases. *J. Biol. Chem.* **282**, 821-825

16. Lenoir, G., Williamson, P., and Holthuis, J. C. (2007) On the origin of lipid asymmetry: the flip side of ion transport. *Curr. Opin. Chem. Biol.* **11**, 654-661

17. Tanaka, K., Fujimura-Kamada, K., and Yamamoto, T. (2011) Functions of phospholipid flippases. *J. Biochem.* **149**, 131-143

18. Sebastian, T. T., Baldridge, R. D., Xu, P., and Graham, T. R. (2012) Phospholipid flippases: building asymmetric membranes and transport vesicles. *Biochim. Biophys. Acta* **1821**, 1068-1077

19. Devaux, P. F., Herrmann, A., Ohlwein, N., and Kozlov, M. M. (2008) How lipid flippases can modulate membrane structure. *Biochim. Biophys. Acta* **1778**, 1591-1600

20. Graham, T. R. and Kozlov, M. M. (2010) Interplay of proteins and lipids in generating membrane curvature. *Curr. Opin. Cell Biol.* **22**, 430-436

21. Natarajan, P., Wang, J., Hua, Z., and Graham, T. R. (2004) Drs2p-coupled aminophospholipid translocase activity in yeast Golgi membranes and relationship to in vivo function. *Proc. Natl. Acad. Sci. USA* **101**, 10614-10619

22. Alder-Baerens, N., Lisman, Q., Luong, L., Pomorski, T., and Holthuis, J. C. (2006) Loss of P4 ATPases Drs2p and Dnf3p disrupts aminophospholipid transport and asymmetry in yeast post-Golgi secretory vesicles. *Mol. Biol. Cell* **17**, 1632-1642

23. Muthusamy, B. P., Natarajan, P., Zhou, X., and Graham, T. R. (2009) Linking phospholipid flippases to vesicle-mediated protein transport. *Biochim. Biophys. Acta* **1791**, 612-619

24. Rose, M. D., Winston, F., and Hieter, P. (1990) *Methods in Yeast Genetics: A Laboratory Course Manual*, Cold Spring Harbor Laboratory Press, Cold Spring Harbor, NY

25. Guthrie, C. and Fink, G. R. (1991) *Guide to Yeast Genetics and Molecular Biology*, Academic Press, San Diego, CA

26. Gietz, R. D. and Woods, R. A. (2002) Transformation of yeast by lithium acetate/single-stranded carrier DNA/polyethylene glycol method. *Methods Enzymol.* **350**, 87-96

27. Elble, R. (1992) A simple and efficient procedure for transformation of yeasts. *Biotechniques* **13**, 18-20

28. Longtine, M. S., McKenzie, A., Demarini, D. J., Shah, N. G., Wach, A., Brachat, A., Philippsen, P., and Pringle, J. R. (1998) Additional modules for versatile and economical PCR-based gene deletion and modification in *Saccharomyces cerevisiae*. *Yeast* **14**, 953-961

29. Takahashi, Y., Fujimura-Kamada, K., Kondo, S., and Tanaka, K. (2011) Isolation and characterization of novel mutations in *CDC50*, the non-catalytic subunit of the Drs2p phospholipid flippase. *J. Biochem.* **149**, 423-432

30. Benjamin, J. J., Poon, P. P., Lewis, S. M., Auger, A., Wong, T. A., Singer, R. A., and Johnston, G. C. (2011) The yeast Arf GTPase-activating protein Age1 is regulated by phospholipase D for post-Golgi vesicular transport. *J. Biol. Chem.* **286**, 5187-5196

31. Lewis, M. J., Nichols, B. J., Prescianotto-Baschong, C., Riezman, H., and Pelham, H. R. (2000) Specific retrieval of the exocytic SNARE Snc1p from early yeast endosomes. *Mol. Biol. Cell* **11**, 23-38

32. Furuta, N., Fujimura-Kamada, K., Saito, K., Yamamoto, T., and Tanaka, K. (2007) Endocytic recycling in yeast is regulated by putative phospholipid translocases and the Ypt31p/32p-Rcy1p pathway. *Mol. Biol. Cell* **18**, 295-312

33. Ireland, L. S., Johnston, G. C., Drebot, M. A., Dhillon, N., DeMaggio, A. J., Hoekstra, M. F., and Singer, R. A. (1994) A member of a novel family of yeast 'Zn-finger' proteins mediates the transition from stationary phase to cell proliferation. *EMBO J.* **13**, 3812-3821

34. Trautwein, M., Schindler, C., Gauss, R., Dengjel, J., Hartmann, E., and Spang, A. (2006) Arf1p, Chs5p and the ChAPs are required for export of specialized cargo from the Golgi. *EMBO J.* **25**, 943-954

35. Wang, C. W., Hamamoto, S., Orci, L., and Schekman, R. (2006) Exomer: A coat complex for transport of select membrane proteins from the trans-Golgi network to the plasma membrane in yeast. *J. Cell Biol.* **174**, 973-983

36. Valdivia, R. H., Baggott, D., Chuang, J. S., and Schekman, R. W. (2002) The yeast clathrin adaptor protein complex 1 is required for the efficient retention of a subset of late Golgi membrane proteins. *Dev. Cell* **2**, 283-294

37. Liu, K., Surendhran, K., Nothwehr, S. F., and Graham, T. R. (2008) P4-ATPase requirement for AP-1/clathrin function in protein transport from the trans-Golgi network and early endosomes. *Mol. Biol. Cell* **19**, 3526-3535

38. Drin, G., Casella, J. F., Gautier, R., Boehmer, T., Schwartz, T. U., and Antonny, B. (2007) A general amphipathic alpha-helical motif for sensing membrane curvature. *Nat. Struct. Mol. Biol.* **14**, 138-146

39. Pranke, I. M., Morello, V., Bigay, J., Gibson, K., Verbavatz, J. M., Antonny, B., and Jackson, C. L. (2011) α-Synuclein and ALPS motifs are membrane curvature sensors whose contrasting chemistry mediates selective vesicle binding. *J. Cell Biol.* **194**, 89-103

40. Zhou, X., and Graham, T. R. (2009) Reconstitution of phospholipid translocase activity with purified Drs2p, a type-IV P-type ATPase from budding yeast. *Proc. Natl. Acad. Sci. USA* **106**, 16586-16591

41. Bigay, J. and Antonny, B. (2012) Curvature, lipid packing, and electrostatics of membrane organelles: defining cellular territories in determining specificity. *Dev. Cell* **23**, 886-895

42. Lewis, S. M., Poon, P. P., Singer, R. A., Johnston, G. C., and Spang, A. (2004) The ArfGAP Glo3 is required for the generation of COPI vesicles. *Mol. Biol. Cell* **15**, 4064-4072

43. East, M. P. and Kahn, R. A. (2011) Models for the functions of Arf GAPs. *Semin. Cell*

Dev. Biol. **22**, 3-9

44. Chen, Y., Sheng, R., Källberg, M., Silkov, A., Tun, M. P., Bhardwaj, N., Kurilova, S., Hall, R. A., Honig, B., Lu, H., and Cho, W. (2012) Genome-wide functional annotation of dual-specificity protein- and lipid-binding modules that regulate protein interactions. *Mol. Cell* **46**, 226-237

45. Ravichandran, K. S., Zhou, M. M., Pratt, J. C., Harlan, J. E., Walk, S. F., Fesik, S. W., and Burakoff, S. J. (1997) Evidence for a requirement for both phospholipid and phosphotyrosine binding via the Shc phosphotyrosine-binding domain *in vivo*. *Mol. Cell. Biol.* **17**, 5540-5549

46. Misu, K., Fujimura-Kamada, K., Ueda, T., Nakano, A., Katoh, H., and Tanaka, K. (2003) Cdc50p, a conserved endosomal membrane protein, controls polarized growth in *Saccharomyces cerevisiae*. *Mol. Biol. Cell* **14**, 730-747

47. Sikorski, R. S., and Hieter, P. (1989) A system of shuttle vectors and yeast host strains designed for efficient manipulation of DNA in *Saccharomyces cerevisiae*. *Genetics* **122**, 19-27

ACKNOWLEDGEMENTS—*I thank our colleagues in the Tanaka laboratory for valuable discussions. I also thank Eriko Itoh for technical assistance. The DLS analysis was carried out with FDLS-3000 at the OPEN FACILITY, Hokkaido University Sousei Hall.*

Table I. Yeast strains used in this study

Strain	Genotype	Reference/source
YKT1066	*MATa lys2-801 ura3-52 his3Δ-200 TRP1 leu2Δ-1*	This study
YKT39	*MATα lys2-801 ura3-52 his3Δ-200 trp1Δ-63 leu2Δ-1*	(46)
YKT1759	*MATa lys2-801 ura3-52 his3Δ-200 trp1Δ-63 leu2Δ-1 KanMX6::P_{GAL1}-GLO3 gcs1Δ::HphMX4*	This study
YKT1760	*MATa lys2-801 ura3-52 his3Δ-200 trp1Δ-63 leu2Δ-1 KanMX6::P_{GAL1}-AGE2 gcs1Δ::HphMX4*	This study
YKT1286	*MATa lys2-801 ura3-52 his3Δ-200 trp1Δ-63 leu2Δ-1 HphMX4::P_{GAL1}-3HA-CDC50 gcs1Δ::KanMX6*	(13)
YKT1631	*MATa lys2-801 ura3-52 his3Δ-200 trp1Δ-63 leu2Δ-1 gcs1Δ::HphMX4*	This study
YKT1761	*MATα lys2-801 his3Δ-200 trp1Δ-63 leu2Δ-1 HphMX4::P_{GAL1}-3HA-CDC50 gcs1Δ::KanMX6 URA3::P_{TPI1}-GFP-SNC1*	This study
YKT1762	*MATa lys2-801 ura3-52 his3Δ-200 trp1Δ-63 leu2Δ-1 gcs1Δ::HphMX4 chs6Δ::KanMX6*	This study
YKT1656	*MATα lys2-801 ura3-52 his3Δ-200 trp1Δ-63 leu2Δ-1 chs6Δ::KanMX4*	(29)
YKT1763	*MATa lys2-801 ura3-52 his3Δ-200 trp1Δ-63 leu2Δ-1 glo3Δ::HphMX4*	This study
YKT1764	*MATa lys2-801 ura3-52 his3Δ-200 TRP1 leu2Δ-1 age2Δ::HphMX4*	This study
YKT1765	*MATa lys2-801 ura3-52 his3Δ-200 trp1Δ-63 leu2Δ-1 glo3Δ::HphMX4 chs6Δ::KanMX6*	This study
YKT1766	*MATa lys2-801 ura3-52 his3Δ-200 TRP1 leu2Δ-1 age2Δ::HphMX4 chs6Δ::KanMX6*	This study
YKT1767	*MATa lys2-801 his3Δ-200 trp1Δ-63 leu2Δ-1 gcs1Δ::KanMX6 URA3::P_{TPI1}-GFP-SNC1*	This study
YKT1768	*MATa lys2-801 ura3-52 his3Δ-200 trp1Δ-63 leu2Δ-1 gcs1Δ::KanMX6*	This study
YKT1769	*MATa lys2-801 ura3-52 his3Δ-200 trp1Δ-63 leu2Δ-1 gcs1Δ::HphMX4 tlg2Δ::KanMX6* pRS416-GFP-GCS1	This study

Table Ⅱ. Plasmids used in this study

Plasmid	Characteristics	Derivation/source
pRS314	*TRP1, CEN6*	(47)
pKT1778 [pRS314-3MYC-GCS1]	P_{GCS1}*-3MYC-GCS1, TRP1, CEN*	This study
pKT1842 [pRS314-3MYC-GCS1 (L246A/W250A /F253A (mutALPS))]	P_{GCS1}*-3MYC-GCS1 (mutALPS), TRP1, CEN6*	This study
pKT1843 [pRS314-3MYC-GCS1 (mutALPS /F292A/F296A)]	P_{GCS1}*-3MYC-GCS1 (mutALPS/F292A/F296A), TRP1, CEN6*	This study
pKT1833 [pRS314-3MYC-GCS1 (F292A/F296A)]	P_{GCS1}*-3MYC-GCS1 (F292A/F296A), TRP1, CEN6*	This study
pKT1777 [pRS314-3MYC-GCS1 (Δ228-279)]	P_{GCS1}*-3MYC-GCS1 (Δ228-279), TRP1, CEN6*	This study
pKT1783 [pRS314-3MYC-GCS1 (Δ228-315)]	P_{GCS1}*-3MYC-GCS1 (Δ228-315), TRP1, CEN6*	This study
pKT1825 [pRS314-3MYC-GCS1 (Δ281-311)]	P_{GCS1}*-3MYC-GCS1 (Δ281-311), TRP1, CEN6*	This study
pKT1852 [pRS314-3MYC-GCS1 (L281A)]	P_{GCS1}*-3MYC-GCS1 (L281A), TRP1, CEN6*	This study
pKT1997 [pRS314-3MYC-GCS1 (mutALPS/L281A)]	P_{GCS1}*-3MYC-GCS1 (mutALPS/L281A), TRP1, CEN6*	This study
pGEX-4T-1	GST (GE Healthcare)	
pKT1937 [pGEX-4T-1-GCS1 (221-352)]	GST-GCS1 (221-352)	This study
pKT1943 [pGEX-4T-1-GCS1 (221-352) mutALPS]	GST-GCS1 (221-352) mutALPS	This study
pKT1942 [pGEX-4T-1-GCS1 (221-352) F292A/F296A]	GST-GCS1(221-352) F292A/F296A	This study
pKT1944 [pGEX-4T-1-GCS1 (221-352) mutALPS/F292A/F296A]	GST-GCS1(221-352) mutALPS/F292A/F296A	This study
pKT1965 [pGEX-4T-1-GCS1 (280-352)]	GST-GCS1 (280-352)	This study
pKT1966 [pGEX-4T-1-GCS1 (280-352) F292A/F296A]	GST-GCS1 (280-352) F292A/F296A	This study
pKT1443 [pRS416-GFP-SNC1]	P_{TPI1}*-GFP-SNC1, URA3, CEN6*	(31)
pKT1564 [pRS416-3HA-SNC1]	P_{TPI1}*-3HA-SNC1, URA3, CEN6*	(32)
pKT1766 [pRS416-GFP-GCS1]	P_{TPI1}*-GFP-GCS1, URA3, CEN6*	This study
pKT1488 [pRS416-GFP-TLG1]	P_{TPI1}*-GFP-TLG1, URA3, CEN6*	This study
pKT2052 [pRS416-2HA-TLG1]	P_{TPI1}*-2HA-TLG1, URA3, CEN6*	This study

Table III. Summary of growth phenotype

Gcs1p derivatives	Cdc50-dep *gcs1*Δ	Glo3-dep *gcs1*Δ	Age2-dep *gcs1*Δ	CW *chs6*Δ *gcs1*Δ	*tlg2*Δ *gcs1*Δ
Vector	−	−	−	−	−
Gcs1	+++	+++	+++	+++	+++
Δ228-279	+++	±	+++	+++	+++
Δ281-311	++	+++	+++	++	++
Δ228-315	−	±	+	−	−
mutALPS	+++	±	+++	+++	+++
F292A/F296A	++	+++	+++	+	+
mutALPS/F292A/F296A	−	±	+	−	−
L281A	+	+++	+++	+	+
mutALPS/L281A	+	±	+++	+	++

−; Lethal, +++; Normal growth

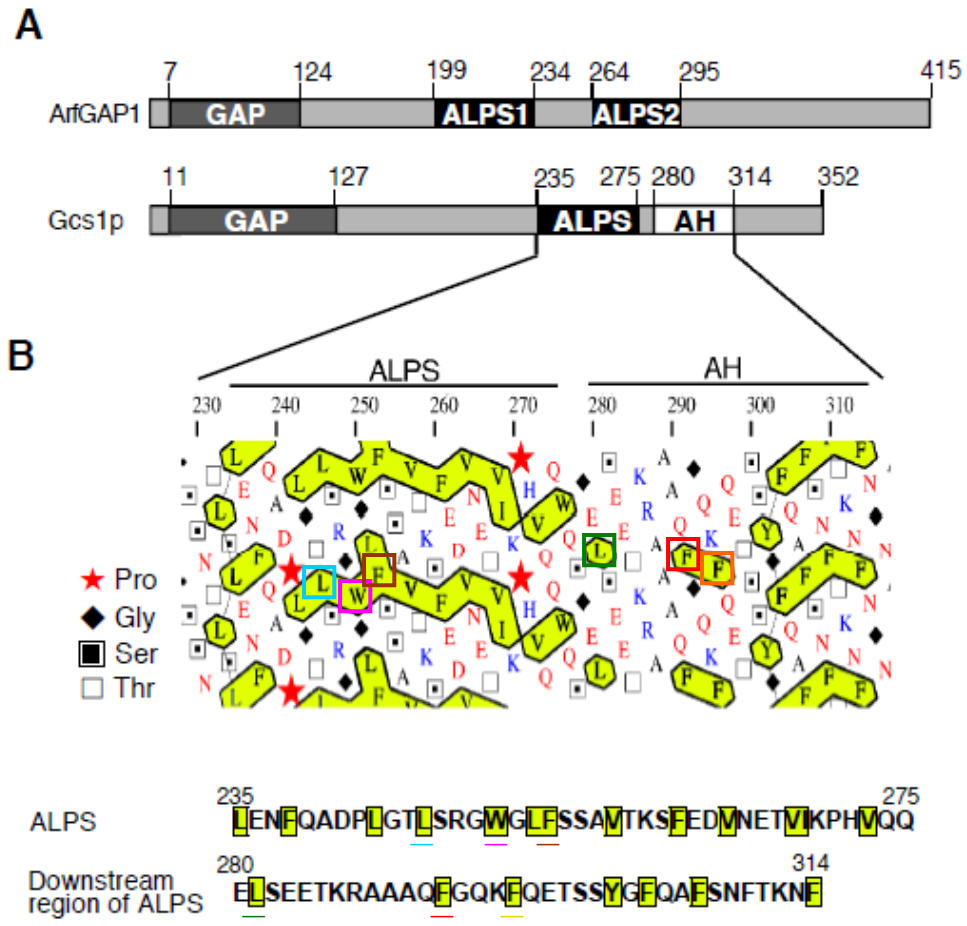
A
ArfGAP1
7
124
199
234
264
295
415
GAP
ALPS1
ALPS2
Gcs1p
11
127
235
275
280
314
352
GAP
ALPS
AH
B
ALPS
AH
230
240
250
260
270
280
290
300
310
Pro
Gly
Ser
Thr
ALPS
235
275
LENFQADPLGTLSRGWGLFSSAVTKSFEDVNETVIKPHVQQ
Downstream region of ALPS
280
314
ELSEETKRAAAQFGQKFQETSSYGFQAFSNFTKNF
C
275
235
314
280
ALPS
Downstream region of ALPS

FIGURE 1. **Existence of a second ALPS-like amphipathic region in Gcs1p.** (A) Domain structures of ArfGAP1 and Gcs1p. AH; amphipathic region. (B) Hydrophobic cluster analysis (HCA) of the region of Gcs1p containing the ALPS motif and its down stream amphipathic region. Hydrophobic clusters are colored yellow. The mutated amino acids are enclosed with square or underlined: ─L246→A, ─W250→A, ─F253→A, ─L281→A, ─F292→A, ─F296→A. (C) Helical wheel projections of the ALPS motif and its downstream region. Hydrophobic, charged, and serine/threonine residues are colored yellow, red, and pink, respectively. The mutated amino acids are the same as that of (B). The web sites for HCA and helical wheel analyses are (http://mobyle.rpbs.univ-paris-diderot.fr/cgi-bin/portal.py?form=HCA#forms::HCA) and (http://150.185.138.86/cgi-bin/emboss/pepwheel), respectively.

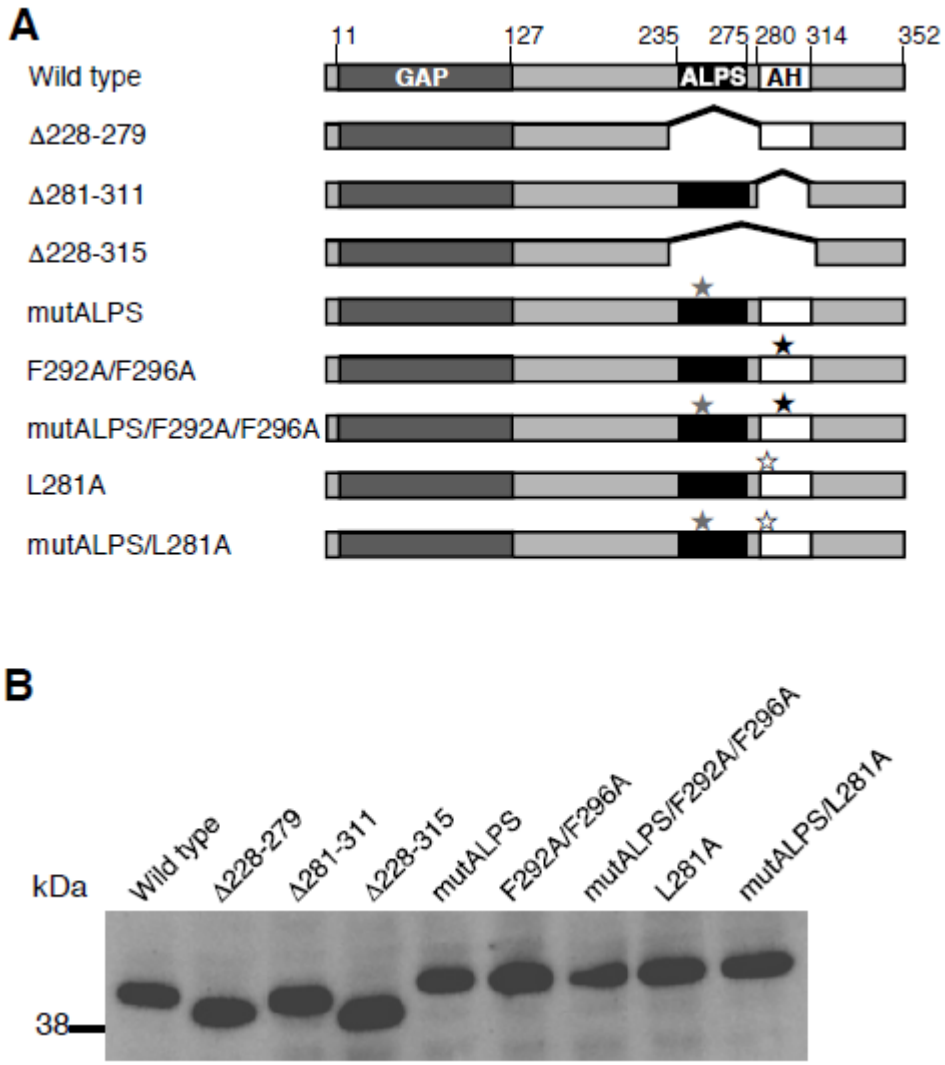

FIGURE 2. **Gcs1p derivatives examined in this study.** All derivatives were expressed under the control of the native promoter from a low copy plasmid. (A) Structures of the Gcs1p derivatives. The gray, black, and open stars indicate mutALPS (L246A/W250A/F253A), F292A/F296A, and L281A mutations, respectively. (B) Protein expression of the Gcs1p derivatives. A *gcs1*Δ strain YKT1631 was transformed with pRS314 plasmids harboring Myc-tagged *GCS1* derivatives. The plasmids used are listed in Table II. Total cell lysates prepared from the cells were subjected to Western blotting with anti-Myc antibody.

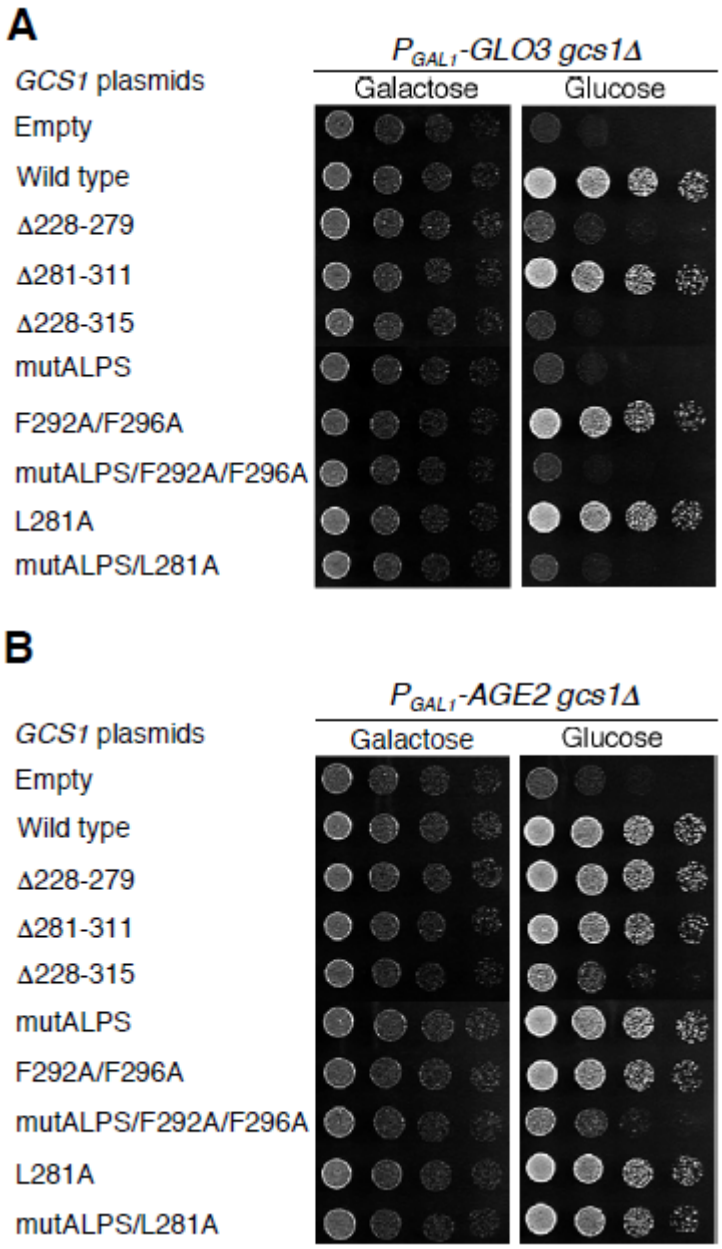

FIGURE 3. **The effect of *GCS1* mutations on the growth property of Glo3p- and Age2p-depleted cells.** YKT1759 (P_{GAL1}-*GLO3 gcs1*Δ) and YKT1760 (P_{GAL1}-*AGE2 gcs1*Δ) were transformed with the *GCS1* mutant plasmids used in Fig. 2. Overnight culture of the transformants was serially diluted and spotted onto YPGA (Galactose) or YPDA (Glucose) plates, followed by incubation at 30°C for 1-2 days.

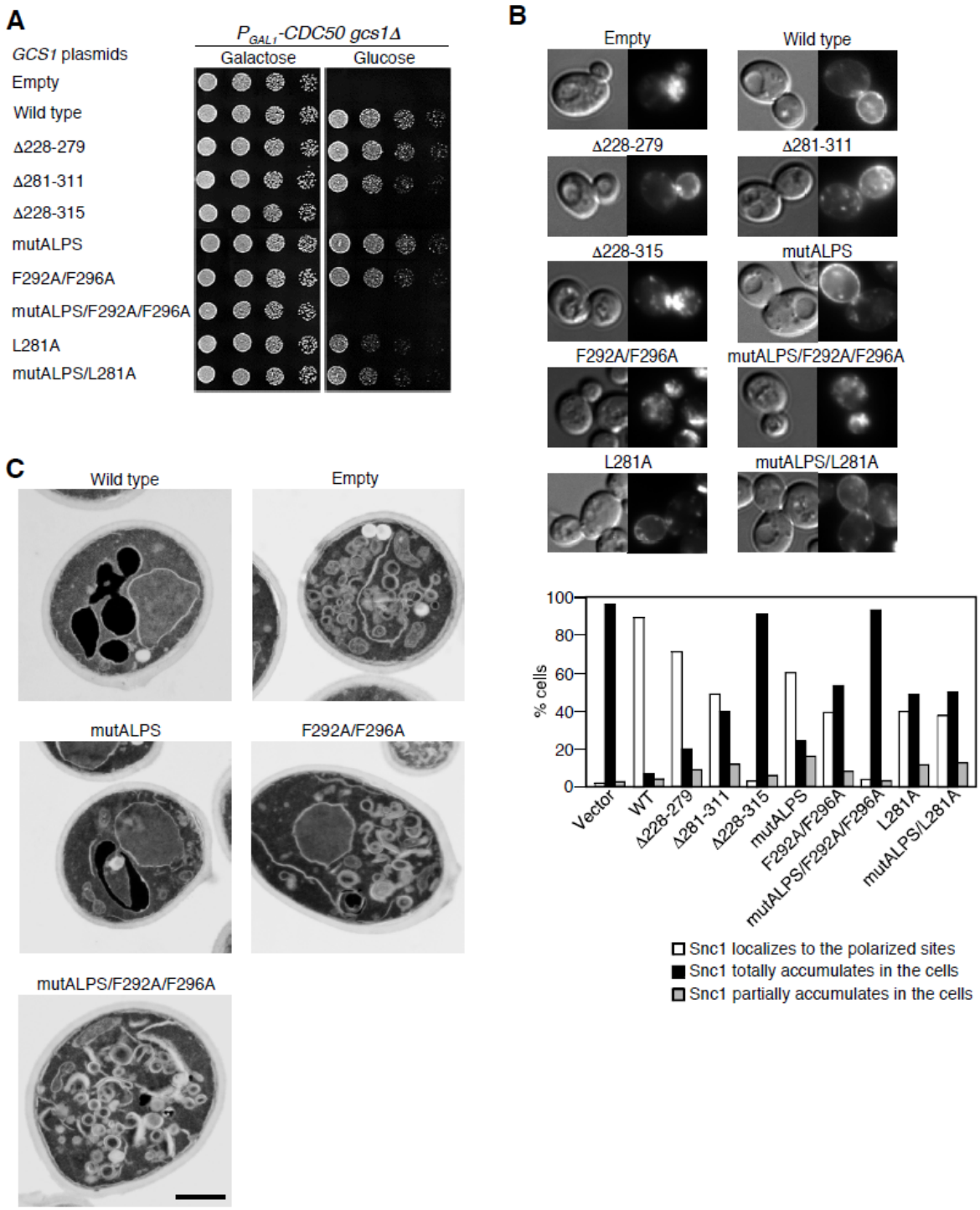
A
P GAL1-CDC50 gcs1Δ
GCS1 plasmids
Galactose
Glucose
Empty
Wild type
Δ228-279
Δ281-311
Δ228-315
mutALPS
F292A/F296A
mutALPS/F292A/F296A
L281A
mutALPS/L281A
B
Empty
Wild type
Δ228-279
Δ281-311
Δ228-315
mutALPS
F292A/F296A
mutALPS/F292A/F296A
L281A
mutALPS/L281A
100
80
60
40
20
0
% cells
Vector
WT
Δ228-279
Δ281-311
Δ228-315
mutALPS
F292A/F296A
mutALPS/F292A/F296A
L281A
mutALPS/L281A
Snc1 localizes to the polarized sites
Snc1 totally accumulates in the cells
Snc1 partially accumulates in the cells
C
Wild type
Empty
mutALPS
F292A/F296A
mutALPS/F292A/F296A

FIGURE 4. **The effect of *GCS1* mutations on the growth property and endocytic recycling of Cdc50p-depleted cells.** (A) The effect on the growth property. P_{GAL1}-*CDC50 gcs1*Δ (YKT1286) cells were transformed with the *GCS1* mutant plasmids used in Fig. 2. Growth of the transformants was examined as in Fig. 3. (B and C) The effect on the endocytic recycling. (B) Localization of GFP-Snc1p in the Cdc50p-depleted *gcs1*Δ mutant bearing Gcs1p derivatives. P_{GAL1}-*CDC50 gcs1*Δ *GFP-SNC1* strain (YKT1761) was transformed with the *GCS1* mutant plasmids used in Fig. 2. The transformant cells were grown at 30°C to early-mid logarithmic phase, followed by incubation in SD medium containing glucose for 7 h, and observed by fluorescence microscopy after fixation. Micrographs of representative cells are shown. The graph shows the percentage of the cells (n>100) categorized for GFP-Snc1 localization sites. (C) Mutations in both ALPS motif and the predicted AH region leads to the accumulation of abnormal membrane structures in the Cdc50p-depleted cells. The transformants used in (A) were grown in YPDA medium at 30°C for 7 h, fixed with glutaraldehyde-osmium, and processed for electron microscopic observation. Bar, 1 μm.

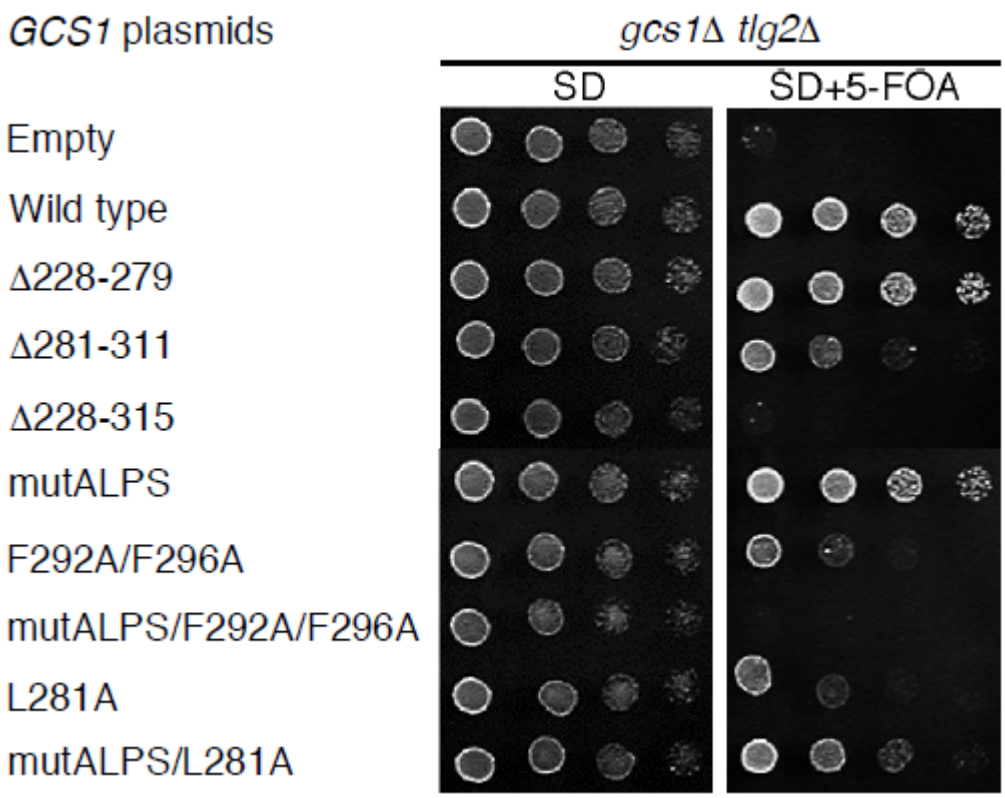

FIGURE 5. **ALPS and the predicted AH region are essential for growth of the *tlg2*Δ mutant.** *gcs1*Δ *tlg2*Δ cells (YKT1769), which were kept alive by the expression of GFP-Gcs1p from a low copy plasmid carrying *URA3* gene (pKT1766), were transformed with the *GCS1* mutant plasmids used in Fig. 2. The *URA3*-containing cells are growth sensitive to 5-FOA, which is converted to toxic 5-fluorouracil by the *URA3* gene product orotidine-5'-phosphate decarboxylase. Thus, if the lethality of the *gcs1*Δ *tlg2*Δ cells is suppressed by the *gcs1* mutant derivatives, the cells can become 5-FOA resistant by losing the GCS1-URA3 plasmid. The transformants were grown at 30°C overnight in SD medium supplemented with uracil to increase cells that lost the *URA3*-containing plasmid, and the cultures were serially diluted and spotted onto SD plates with or without 5-FOA, followed by incubation at 30°C for 1-2 days.

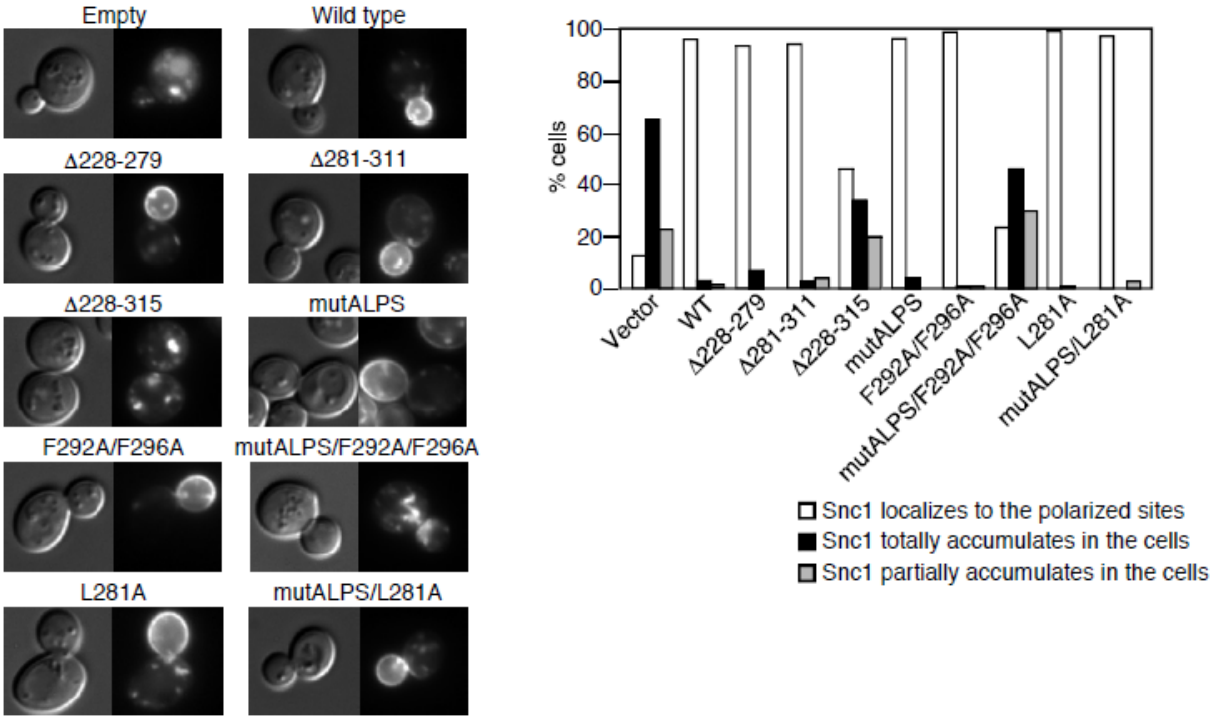

FIGURE 6. **The effect of *GCS1* mutations on the endocytic recycling of GFP-Snc1p at a low temperature.** *gcs1*Δ *GFP-SNC1* cells (YKT1767) were transformed with the *GCS1* mutant plasmids used in Fig. 2. The transformant cells were grown in SD medium at 14°C for more than 18 h, and observed immediately by fluorescence microscopy. Micrographs of representative cells are shown. The graph shows the percentage of the cells (n>100) categorized for GFP-Snc1p localization sites.

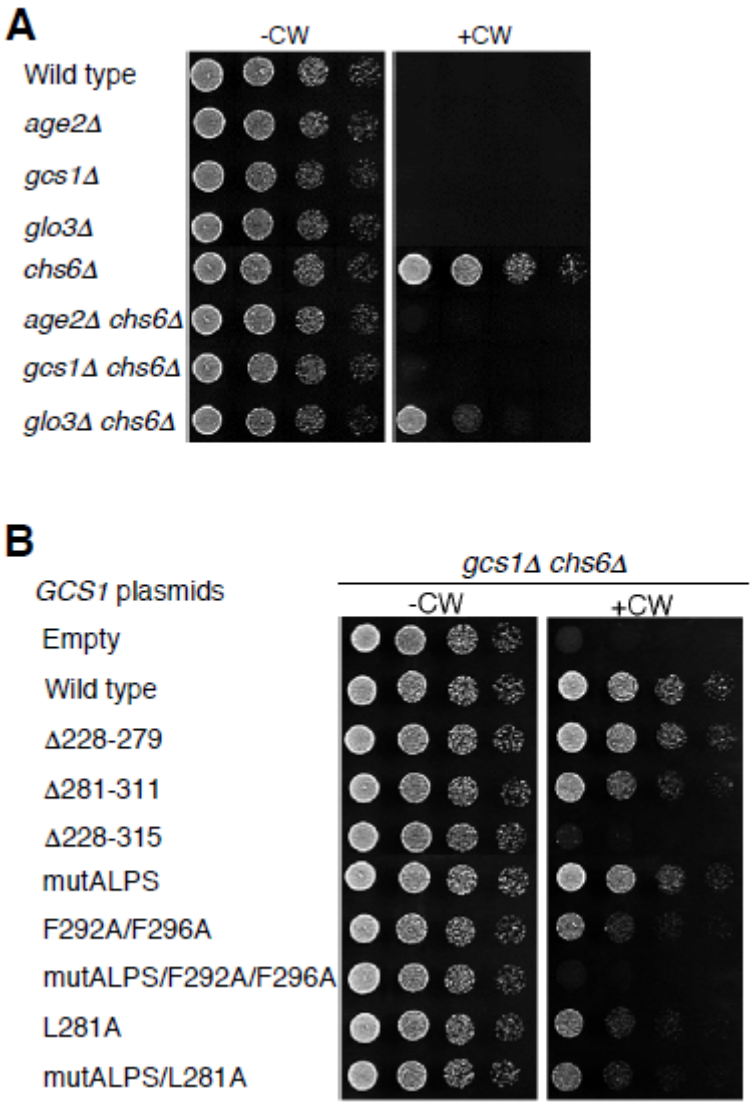

FIGURE 7. **Mutations in ArfGAPs or the ALPS and predicted AH region of Gcs1p restore the plasma membrane localization of Chs3p.** (A) Disruption of ArfGAPs restores calcofluor sensitivity of *chs6*Δ cells. Overnight culture of the cells was serially diluted and spotted onto YPDA plates supplemented with (+CW) or without (-CW) 100 μg/ml calcofluor, followed by incubation at 30°C for 1 day. Strains used were: YKT1066 (WT), YKT1764 (*age2*Δ), YKT1631 (*gcs1*Δ), YKT1763 (*glo3*Δ), YKT1656 (*chs6*Δ), YKT1766 (*age2*Δ *chs6*Δ), YKT1762 (*gcs1*Δ *chs6*Δ), YKT1765 (*glo3*Δ *chs6*Δ). (B) Mutations in the ALPS and predicted AH region of Gcs1p

restore calcofluor sensitivity of *chs6*Δ cells. *gcs1*Δ *chs6*Δ strain (YKT1762) was transformed with the *GCS1* mutant plasmids used in Fig. 2. Calcofluor sensitivity was examined as in (A).

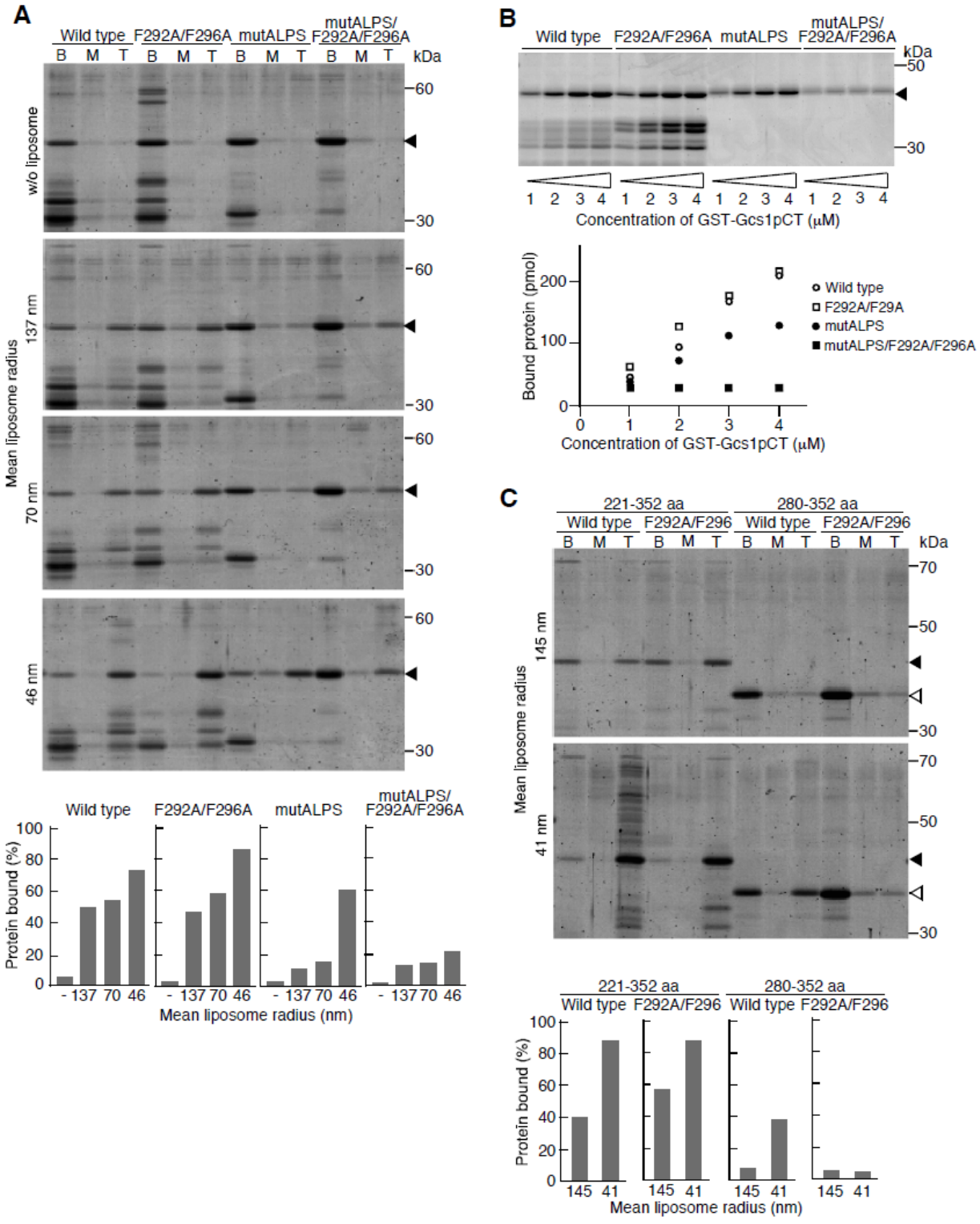
A
Wild type
F292A/F296A
mutALPS
mutALPS/
F292A/F296A
B M T
kDa
w/o liposome
137 nm
70 nm
46 nm
Mean liposome radius
60
30
Protein bound (%)
Mean liposome radius (nm)
- 137 70 46
B
Concentration of GST-Gcs1pCT (μM)
Bound protein (pmol)
Wild type
F292A/F29A
mutALPS
mutALPS/F292A/F296A
C
221-352 aa
280-352 aa
145 nm
41 nm
145 41

FIGURE 8. **The predicted AH region is capable of sensing the membrane curvature.** (A) Binding of GST-Gcs1p(221-352) to liposomes is dependent on the ALPS and predicted AH region. GST-fused Gcs1p(221-352) proteins (1.5 μM) carrying amino acid substitutions in the ALPS (mutALPS) or/and the predicted AH region (F292A/F296A) were examined for binding to Golgi-mix liposomes of various size (1 mM lipids) by liposome flotation assay as described in the Materials and methods. T, M, and B indicate top, middle, and bottom fractions, respectively. The Gcs1p(221-352) proteins are indicated with arrowheads. The ratio of protein recovered in the top fraction was expressed as a percentage of the protein bound to liposomes (bottom panel). (B) Dose-dependent binding of the GST-Gcs1p(221-352) mutant proteins to the liposome. Liposome flotation assay was performed as in (A) for 37 nm liposome with various concentrations (1~4 μM) of GST-Gcs1p(221-352) mutant proteins. Only the top fractions are shown. The amount of proteins bound to liposomes (pmol) was plotted against protein concentration (bottom panel). (C) Binding of the predicted AH region to small size liposomes. GST-Gcs1p(280-352) and its F292A/F296A mutant containing only the predicted AH region were examined for liposome binding as in (A) (open arrowheads) with GST-Gcs1p(221-352) versions containing both ALPS and the predicted AH region as controls (arrowheads).

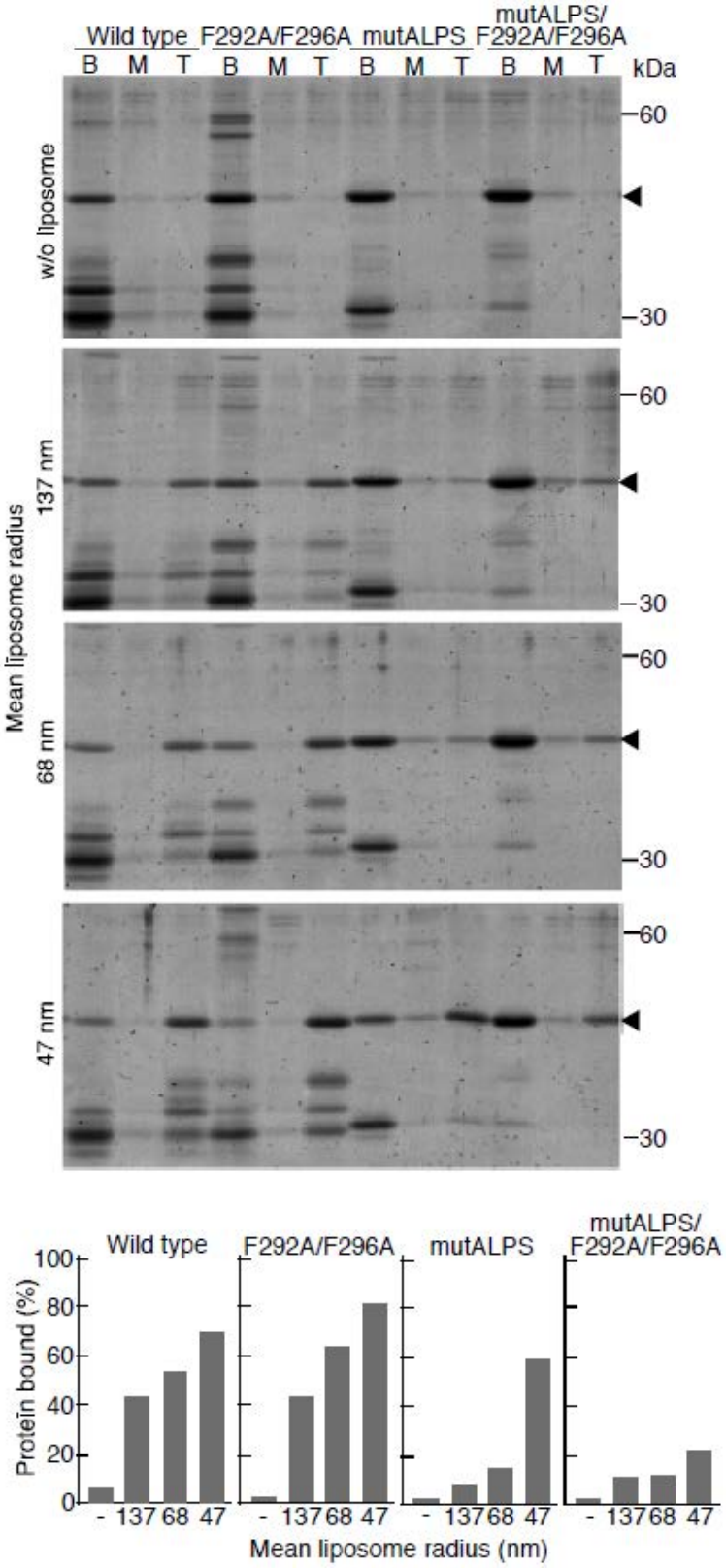
Wild type
F292A/F296A
mutALPS
mutALPS/
F292A/F296A
B M T B M T B M T B M T
kDa
w/o liposome
137 nm
68 nm
47 nm
Mean liposome radius
60
30
Protein bound (%)
100
80
60
40
20
0
- 137 68 47
Mean liposome radius (nm)

FIGURE 9. **PS dose not affect the liposome binding property of GST-Gcs1p(221-352) and its mutant proteins.** The liposome flotation assay was performed as in Fig. 8A, except that PS was replaced with PC in the Golgi-mix liposomes (0% DOPS and 55% DOPC).

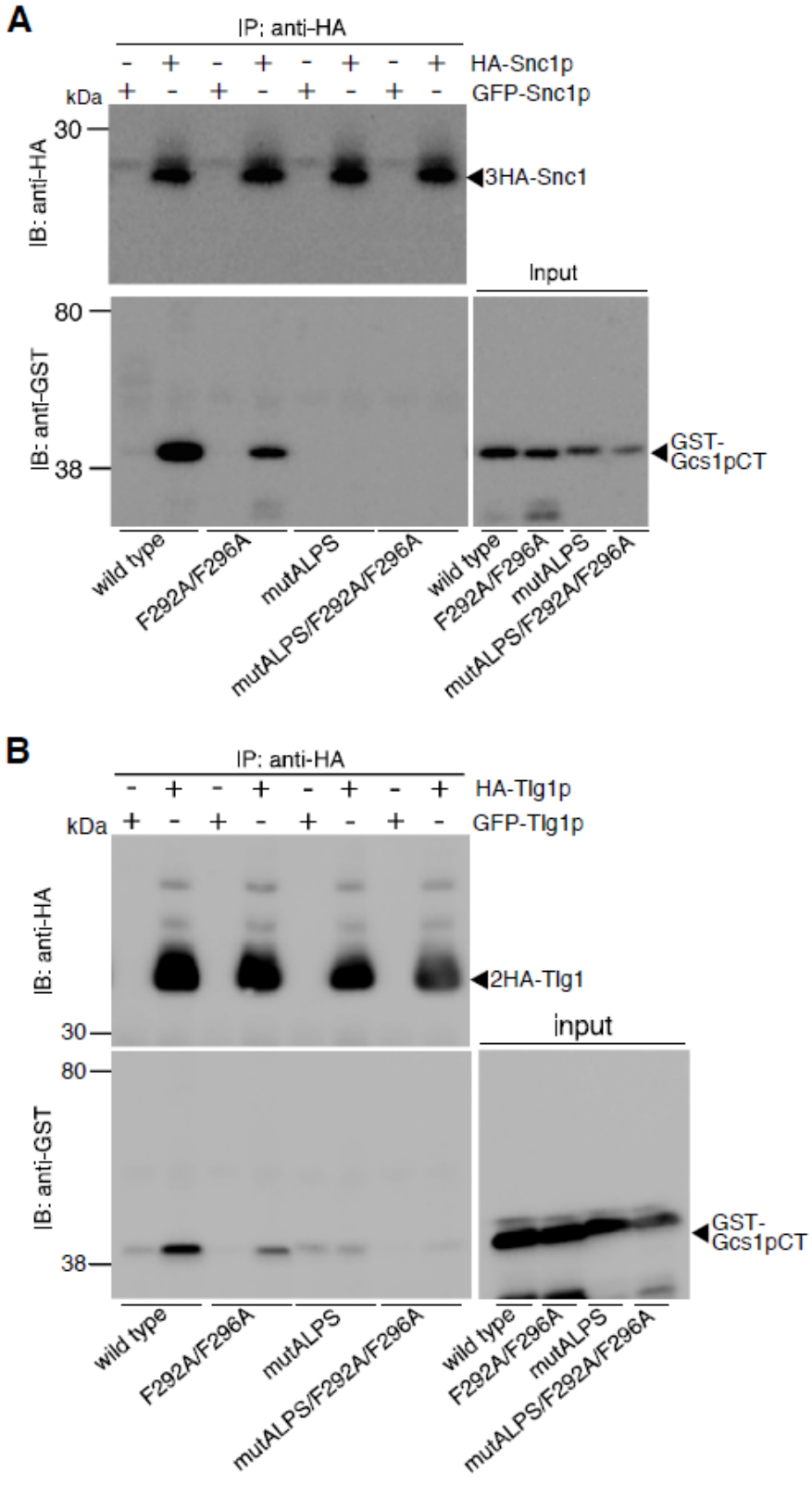
A
IP: anti-HA
HA-Snc1p
GFP-Snc1p
kDa
30
IB: anti-HA
3HA-Snc1
Input
80
IB: anti-GST
38
GST-
Gcs1pCT
wild type
F292A/F296A
mutALPS
mutALPS/F292A/F296A
B
IP: anti-HA
HA-Tlg1p
GFP-Tlg1p
kDa
IB: anti-HA
2HA-Tlg1
30
Input
80
IB: anti-GST
38
GST-
Gcs1pCT
wild type
F292A/F296A
mutALPS
mutALPS/F292A/F296A

FIGURE 10. **Contribution of the ALPS motif to the interaction with Snc1p and Tlg1p.** (A) Interaction of GST-Gcs1p(221-352) and its mutant proteins with HA-Snc1p. HA-Snc1p immunoprecipitated from the membrane protein extracts of *gcs1*Δ cells (YKT1768) containing pRS416-3HA-SNC1 (pKT1564) was tested for binding to GST-Gcs1p(221-352) and its mutant proteins as described in Materials and methods. *gcs1*Δ cells containing pRS416-GFP-SNC1 (pKT1443) were used as a control. (B) Interaction of GST-Gcs1p(221-352) and its mutant proteins with HA-Tlg1p. Experiments were performed as in (A) with *gcs1*Δ cells containing pRS416-2HA-TLG1 (pKT2052) or pRS416 -GFP-TLG1 (pKT1488).

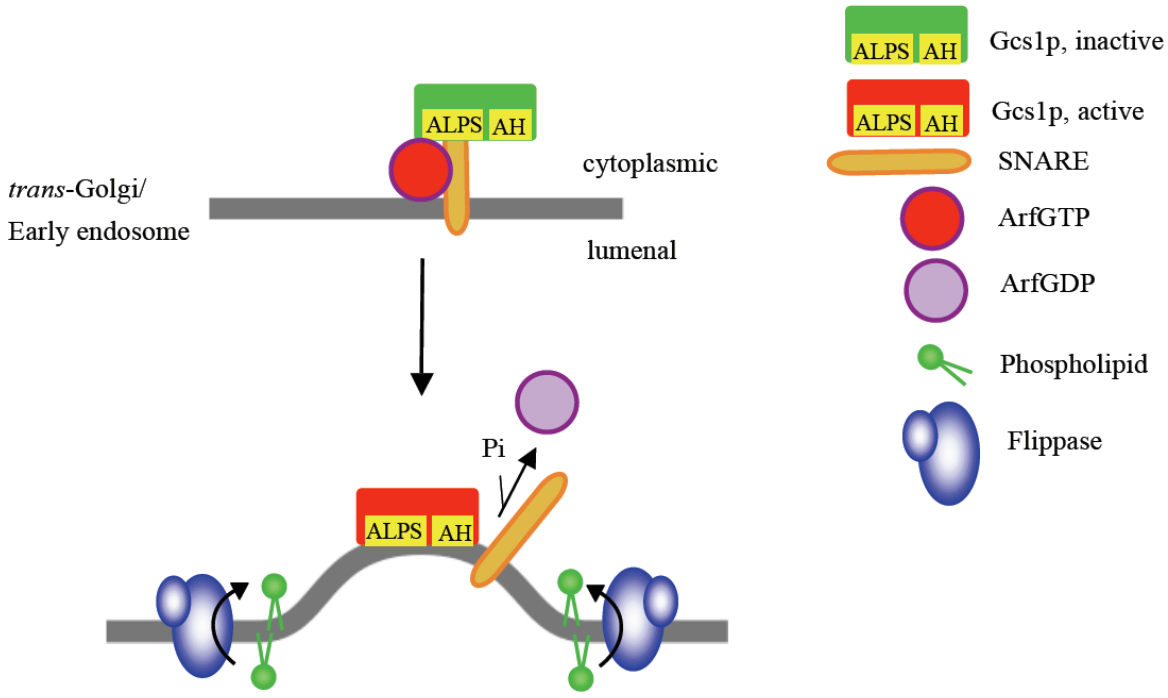

FIGURE 11. **A predicted model for the contribution of ALPS and AH to the Gcs1p function in vesicle biogenesis.**